**LETTER**

# Spread of consensus in self-organized groups of individuals: Hydrodynamics matters

To cite this article: A. De Rosis *et al* 2016 *EPL* **113** 18001

A LETTERS JOURNAL EXPLORING
THE FRONTIERS OF PHYSICS

January 2016

EPL, **113** (2016) 18001
doi: 10.1209/0295-5075/113/18001

www.epljournal.org

# Spread of consensus in self-organized groups of individuals: Hydrodynamics matters

A. DE ROSIS[1], E. LÉVÊQUE[1], S. UBERTINI[2] and S. SUCCI[3]

[1] *Laboratoire de Mécanique des Fluides et d'Acoustique, Ecole Centrale de Lyon - 36 avenue Guy de Collongue, 69134 Ecully cedex, France*
[2] *Industrial Engineering School, University of Tuscia - Largo dell'Universitá s.n.c., 01100, Viterbo, Italy*
[3] *Istituto per le Applicazioni di Calcolo, CNR - Via dei Taurini 19, 00185, Rome, Italy*

received 25 September 2015; accepted in final form 7 January 2016
published online 26 January 2016

PACS 89.75.Fb – Structures and organization in complex systems
PACS 05.65.+b – Self-organized systems

**Abstract** – Nature routinely presents us with spectacular demonstrations of organization and orchestrated motion in living species. Efficient information transfer among the individuals is known to be instrumental to the emergence of spatial patterns (*e.g.* V-shaped formations for birds or diamond-like shapes for fishes), responding to a specific functional goal such as predatory avoidance or energy savings. Such functional patterns materialize whenever individuals appoint one of them as a leader with the task of guiding the group towards a prescribed target destination. It is here shown that, under specific conditions, the surrounding hydrodynamics plays a critical role in shaping up a successful group dynamics to reach the desired target.



**Introduction.** – The migration of a group of active agents, such as flocks of birds, schools of fishes, swarms of insects and humans as well [1–12], towards a given target destination is a process in which a given portion of the group is informed about the route, and transfers this information to the naive ones through social behavioural interactions [13–19]. Information transfer within a school of fishes has been investigated in [16,19], showing that a quorum of informed individuals is required to facilitate a group coherence. In addition, Ballerini *et al.* [20] observed that the collective behaviour of birds involves topological aspects, accounting only for the presence of the nearest neighbours. At a lower size scale, experimental evidences in [21] show that the cohesion in a group of midges is enhanced by the presence of some interaction-induced effective forces. Obviously, the deep understanding of the dynamics of a group of animals which have identified and follow a leader is an intriguing issue, with potentially far-reaching consequences. For instance, it has been shown that a robotic fish drone can guide real organisms by beating its tail at a particular frequency [22]. Suppose one would aim at designing an artificial leader capable of persuading a certain number of individuals, a natural question is: how can the persuasive performance of the robot be affected by external inputs relative to the surrounding fluid environment? In the present study, we show that whenever the numbers of informed and uninformed individuals are of the same order of magnitude, hydrodynamics may play a crucial role on the decision-making process of the individuals.

**Methods.** – Here, we analyse the effects of hydrodynamics in the collective behaviour of a group of agents for low Reynolds numbers, representative of various life scenarios [23]. The rules governing the mutual interaction between the individuals have been implemented in two dimensions according to the so-called agent-based collective behavioural model proposed by Couzin [24]. Each agent identifies two concentric regions as sketched in fig. 1. On the one hand, the inner region is a circular repulsion zone with radius $l_r$. If a generic individual, $j$, detects another individual, $k$, in this zone, it varies its own direction in order to avoid collision. On the other hand, the outer zone is an attraction-orientation area. It covers a circular zone with radius $l_{a,o} - l_r$. If an individual $k$ is found here moving in a certain direction, the generic individual $j$ tends to move closer to this latter and take the same orientation. To instil information about the route, some (informed) individuals adapt their direction to reach a prescribed target point. Accordingly, at each time instant $t$ the generic

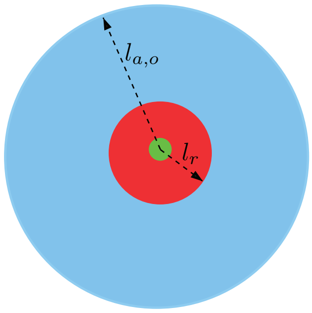


Fig. 1: (Colour online) Schematic representation of the zone-based model. Each individual (green circle) is surrounded by two areas: the repulsion one (red circle of radius $l_r$) and the attraction-orientation one (light blue circle of radius $l_{a,o}$).

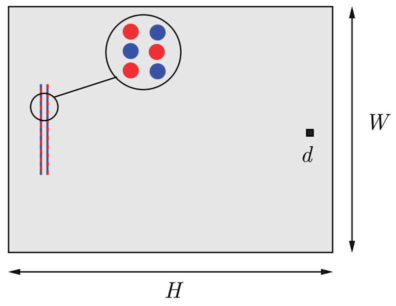


Fig. 2: (Colour online) Sketch of the problem set-up. $H = 900$, $W = 600$. The prescribed target (black point, $d$) is located at 700 grid nodes from the leftmost surface. The rightmost column of individuals is located at 200 grid nodes from the leftmost surface. Informed (red) and naive (light blue) agents are uniformly distributed.

individual $j$ updates the direction of its velocity vector $\boldsymbol{V}_j$, and its position $\boldsymbol{X}_j$, as follows:

$$\boldsymbol{V}_j(t) = \boldsymbol{V}_j^r(t) + \boldsymbol{V}_j^{a,o}(t) + \boldsymbol{V}_j^d(t), \tag{1}$$

$$\boldsymbol{X}_j(t+\Delta t) = \boldsymbol{X}_j(t) + \frac{\boldsymbol{V}_j(t)}{|\boldsymbol{V}_j(t)|} U \Delta t, \tag{2}$$

where

$$\boldsymbol{V}_j^r(t) = -\sum_{k \neq j} \boldsymbol{r}_{j,k}, \quad \text{if } \boldsymbol{r}_{j,k} \leq l_r, \tag{3}$$

$$\boldsymbol{V}_j^{a,o}(t) = w_a \sum_{k \neq j} \boldsymbol{r}_{j,k} + w_o \sum_k \frac{\boldsymbol{V}_k}{|\boldsymbol{V}_k|}, \quad \text{if } l_r < \boldsymbol{r}_{j,k} \leq l_{a,o}, \tag{4}$$

$$\boldsymbol{V}_j^d(t) = \boldsymbol{r}_{j,d}, \quad \text{if } j \text{ is informed}, \tag{5}$$

where $\Delta t$ is the time step, $U$ is a characteristic cruising speed, $\boldsymbol{r}_{j,k} = \frac{\boldsymbol{X}_k - \boldsymbol{X}_j}{|\boldsymbol{X}_k - \boldsymbol{X}_j|}$ is the normalized distance between the individuals $j$ and $k$, $\boldsymbol{V}_k$ is the velocity vector of the individual $k$ and $\boldsymbol{r}_{j,d} = \frac{\boldsymbol{X}_d - \boldsymbol{X}_j}{|\boldsymbol{X}_d - \boldsymbol{X}_j|}$ is the normalized distance between the position of the individual $j$ and the destination (target) point, $d$.

The above equations are purely *kinematic* and independent of physical aspects such as the individuals' inertia (mass and shape), or the force interaction with the encompassing medium (*e.g.* air, water). These issues related to *kinetics* are addressed here, where the group (composed of individuals of mass $m$) sets in motion an unbounded fluid domain with kinematic viscosity $\nu$ and mass density $\rho$. Our aim is to highlight the impact of the surrounding hydrodynamics on the decision-making process, and elucidate how the transfer of information between individuals and the spread of a global consensus can be altered by the medium. The motion of each individual obeys Newton's law

$$m \frac{\mathrm{d}^2 \boldsymbol{X}_j}{\mathrm{d}t^2} = \boldsymbol{F}_j, \tag{6}$$

where $\boldsymbol{F}_j$ denotes the force due to the surrounding fluid. The advance in time of the position of the individuals is now achieved through a predictor-corrector scheme, in which behavioural interactions (eqs. (1)–(5)) yield a hydrodynamic-free prediction of the new positions, then corrected by accounting for the fluid forces (eq. (6)). The fluid dynamics, governed by the Navier-Stokes equations, is numerically computed on a regular grid by the lattice Boltzmann method [25], and the presence of the moving individuals is accounted by an immersed boundary algorithm [26,27]. In our problem, the reference length scale is given by the elementary scale of hydrodynamics (the size of a grid cell), whereas the reference time scale results from the "CFL condition" of the lattice Boltzmann method [25]; the reference mass density is provided by the fluid density. In the following, quantities will be given in dimensionless units relative to these characteristic scales. The individuals are modelled as circular solid bodies of radius $r = 1$ and mass $m = 10$. The size of the repulsion zone is $l_r = 4r$, while the attraction-orientation zone extends to $l_{a,o} = 8l_r$. Attraction and orientation tendencies are differently weighted with $w_a = 0.3$ and $w_o = 0.7$ in eq. (4). In this way, the attitude of the individuals to get reciprocally aligned is promoted compared to the perspective to create a compact pattern. This is consistent with the recent observations [24]. The cruising speed is set to $U = 0.02$ and the time step is $\Delta t = 1$. The individuals are initially aligned in two parallel identical columns, whose horizontal spacing is set to $l_r$ (see fig. 2).

**Results and discussion.** – Scenarios characterized by different values of the number of individuals, $\mathcal{N}$, are examined with $10 \leq \mathcal{N} \leq 100$. Among the individuals, only half of them are informed to move towards a prescribed target according to eq. (5). Further details about problems set-up are given in fig. 2. Different values of the Reynolds number ($\mathcal{R}e \in [0.12–1.2]$) based on the diameter of the individuals and the cruising speed are adopted, which are achieved by varying the fluid kinematic viscosity. The idea is here to investigate some possible dependences of the group dynamics on the flow regime. To highlight the effect of hydrodynamics, scenarios neglecting this latter

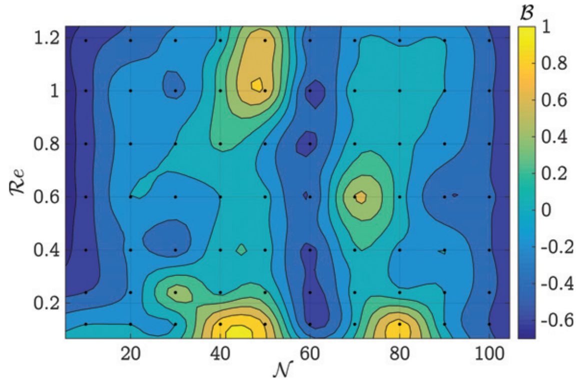


Fig. 3: (Colour online) Map of the hydrodynamic benefit function $\mathcal{B}$: interpolated contour map. 50% of the group is informed.

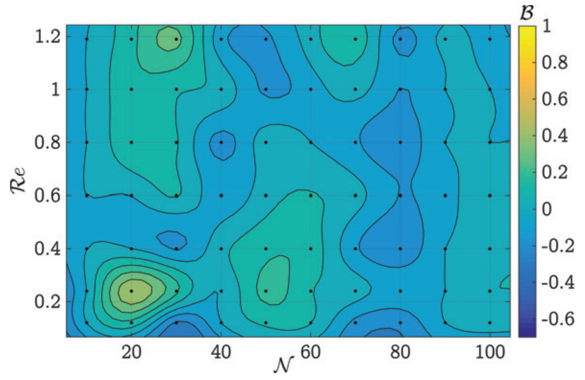


Fig. 4: (Colour online) Map of the hydrodynamic benefit function $\mathcal{B}$: interpolated contour map. 30% of the group is informed.

have been also investigated. A "benefit function" is introduced as

$$\mathcal{B} = \frac{\mathcal{N}^h - \mathcal{N}^{n,h}}{\mathcal{N}^{n,h}}, \tag{7}$$

where $\mathcal{N}^h$ and $\mathcal{N}^{n,h}$ denote the number of individuals reaching the target by accounting for and neglecting the hydrodynamics, respectively. In fig. 3, the value of $\mathcal{B}$ is plotted against $\mathcal{R}e$ and $\mathcal{N}$ and a strong non-linear dependence is observed. On the one hand, the hydrodynamics plays a deleterious role for the extreme values of the size of the group. On the other hand, two zones are identified, *i.e.* $40 \leq \mathcal{N} \leq 50$ and $70 \leq \mathcal{N} \leq 80$, thus highlighting that here the fluid presence enhances the spread of a global consensus within the group. Interestingly, these latter regions of the $\mathcal{B}$ contour map are separated by the configurations at $\mathcal{N} = 60$, which are markedly negative. Finally, we notice that the incidence of $\mathcal{R}e$ is prominent if the group is composed by 30 individuals. In fact, it is possible to observe that for the lowest values of $\mathcal{R}e$ the hydrodynamics enforces a more cohesive group, while presenting deleterious effects as $\mathcal{R}e$ grows. The marked non-linear dependence of $\mathcal{B}$ on $\mathcal{N}$ and $\mathcal{R}e$ is confirmed in fig. 4, where the benefit function is depicted in configurations where 30% of the group is informed. Differently from fig. 3 where vertical stripes of hydrodynamics benefit appear, here the hydrodynamic benefit is confined to local spots. Interestingly, scenarios characterized by $\mathcal{N} = 30$ are, again, those exhibiting the larger sensitivity to the Reynolds number. In fig. 5, the values of $\mathcal{B}$ are reported for tests involving a larger population size, *i.e.* $\mathcal{N} = 150$. By increasing the size of the group, the compelling dependence on the encompassing fluid dynamics still persists. It is worth noting that the effect of the fraction of informed agents is more prominent for low values of $\mathcal{R}e$. On the contrary, we repeated the simulations by assigning the information about the route only to 10% of the set of individuals and found that the uninformed portion is unable to reach the goal, independently of $\mathcal{N}$ and $\mathcal{R}e$. Hydrodynamics does not help to lead the group to the target when the fraction of informed individuals is too small.

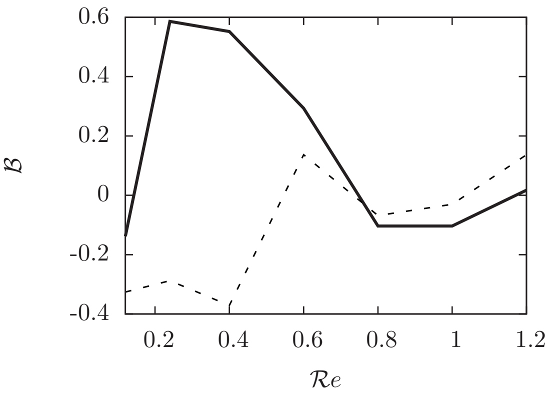


Fig. 5: $\mathcal{B}$ *vs.* $\mathcal{R}e$. Findings are representative of scenarios where 30% (continuous line) and 50% (dashed line) of the agents is informed for a group composed of 150 individuals.

Some insight into this non-linear behaviour can be gained by investigating the time evolution of the spatial position taken by the informed and naive individuals[1]. Specifically, the scenarios characterized by $\mathcal{N} = 50$ are considered and half of the group is assumed to be informed. In fig. 6 (without hydrodynamics), the position of the individuals is reported at three time instants, *i.e.* $t = 1250$, 7500, and 15000. Red and blue circles denote informed and naive agents, respectively. At the earlier stage, about half of the informed individuals moves resolutely towards the target. As the simulation proceeds, naive individuals get partially influenced by the informed subset. Eventually, only four individuals manage to join the informed group, whereas the others lose contact and get disoriented. These effects are emphasized once the hydrodynamics is considered. In fig. 7, the spatial position is depicted at $\mathcal{R}e = 0.24$. At the beginning of the simulation, the group is more compact with respect to the

[1]Some supplementary animations depicting the space-time evolution of the agents, together with the velocity field of the encompassing fluid, are provided: `n10_hydro.avi`, `n50_hydro.avi`, `n100_hydro.avi`, `n10_nohydro.avi`, `n50_nohydro.avi`, `n100_nohydro.avi`.

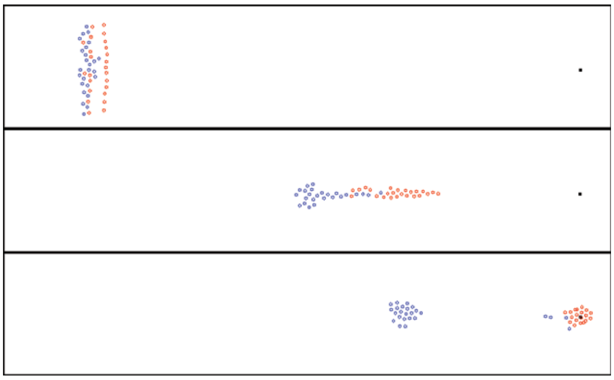

Fig. 6: (Colour online) In the absence of hydrodynamics: position achieved by informed (red) and naive (blue) individuals at different time instants, *i.e.* $t = 1250$ (top), 7500 (middle) and 15000 (bottom). The black point represents the target.

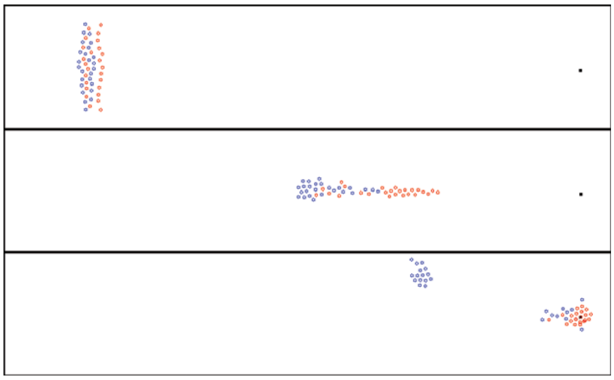

Fig. 7: (Colour online) In the presence of hydrodynamics: position achieved by informed (red) and naive (blue) individuals at different time instants, *i.e.* $t = 1250$ (top), 7500 (middle) and 15000 (bottom) for $\mathcal{R}e = 0.24$. The black point represents the target.

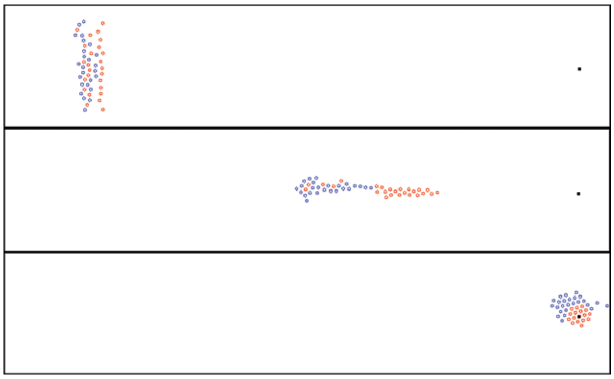

Fig. 8: (Colour online) In the presence of hydrodynamics: position achieved by informed (red) and naive (blue) individuals at different time instants, *i.e.* $t = 1250$ (top), 7500 (middle) and 15000 (bottom) for $\mathcal{R}e = 1.2$. The black point represents the target.

previous scenario. This should be attributed to the initial resistance to the motion exerted by the surrounding quiescent viscous fluid. At the second instant, three subgroups may be identified. At the front, informed individuals lead the group, whereas naive individuals lag behind. In between, an elongated aggregate of both informed and naive individuals has formed. These individuals will eventually reach the target together with the head. What happens at $\mathcal{R}e = 1.2$ (see fig. 8) is intriguing. Again, three subgroups can be identified, but there are important differences. In the trailing part, informed individuals are more diffused among the naive ones. A huge portion of the naive individuals are bounded between the heading and trailing informed agents. Two benefits can be immediately identified. Firstly, since in the left part some informed individuals are present, no fully-uninformed region manifests. This means that each naive receives the information about the route. Secondly, in the central part naive individuals gain information both from the heading part and from the informed neighbours. In this way, the spread of information is widely and extensively disseminated among the whole group, which will successfully reach the target. Therefore, the non-linear shape dynamics forges a complex $\mathcal{B}$ landscape. Finally, in order to account for random perturbations from the environment, we have carried out a Monte Carlo analysis for each $\mathcal{R}e$-$\mathcal{N}$ combination consisting of 1000 runs. Specifically, noise is added by rotating each individual direction, $\boldsymbol{V}_j$, by a random angle drawn from a normal distribution. For the parameter regime explored in this work, *i.e.* a variance up to 0.1 (radians), the noise was not found to lead to any appreciable effect, as it just reduces to a small scatter around the mean value, pretty close to the deterministic (noise-free) result.

A final remark should be devoted to the role of initial conditions. In particular, we have investigated an additional configuration where individuals show homogeneously mixed initial locations with the same typical distance between surrounding individuals inside a hexagon. Our attention focused on scenarios characterized by $\mathcal{N} = 30$ and 60 when half of the group is informed. We have chosen these configurations as representative of different collective dynamics: the former shows the highest variation with $\mathcal{R}e$, whereas the second indicates a general deleterious effect of the hydrodynamics. Making reference to fig. 9 and fig. 10, a dependence on the initial conditions is confirmed. If these are responsible for patterns where informed and naive agents are well mixed, a benefit arises in terms of global consensus. Figure 9 (corresponding to $\mathcal{N} = 30$) shows values of $\mathcal{B}$ chracterized by a high sensitivity to $\mathcal{R}e$. More interesting findings are shown in fig. 10, where it is observed that the different initial conditions drastically modify the hydrodynamic benefit function when the group is composed of 60 agents. On the one hand, hydrodynamics plays a detrimental role in the double-column alignment. On the other hand, fluid forces enhance the spread of consensus within the group if a hexagonal initial arrangement is considered.

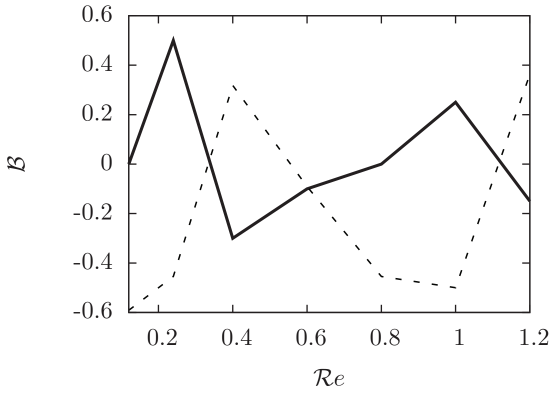


Fig. 9: $\mathcal{N} = 30$: $\mathcal{B}$ *vs.* $\mathcal{R}e$ for double-column (continuous line) and hexagonal (dashed line) arrangements.

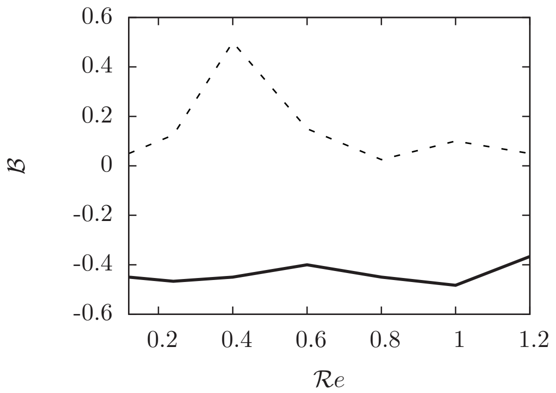


Fig. 10: $\mathcal{N} = 60$: $\mathcal{B}$ *vs.* $\mathcal{R}e$ for double-column (continuous line) and hexagonal (dashed line) arrangements.

**Conclusions.** – In summary, we found that the decision-making process in a group of self-organized individuals is non-trivially altered by the induced motion of the surrounding medium. Specifically, a strong non-linear dependence of the number of individuals reaching the target on $\mathcal{R}e$ and $\mathcal{N}$ has been found for low values of $\mathcal{R}e$ ($\mathcal{R}e \in [0.12–1.2]$). This tendency has to be attributed to the fact that the fluid forces clearly modify the spatial position of the individuals within the group. Consistently, if it leads to patterns where naive and informed agents are well assorted, a more marked spread of information arises. In that case, global consensus drastically grows and a larger portion of the group reaches the prescribed target. This offers a remarkable example of synergistic coupling between social interactions and non-linear hydrodynamics. The insights developed in this work may prove useful for practical applications in several areas of modern science and bio-engineering, such as communication-driven collective motion [28] and nanomedical applications [29,30]. Further analyses to extend the present study to higher Reynolds numbers are in progress. Eventually, a parametric study to predict the minimum number of individuals that should be convinced in order to generate global consensus is under investigation by systematically varying relevant quantities (*i.e.* $\mathcal{R}e$, $\mathcal{N}$, fraction of informed agents).

* * *

This work was done in the framework of the "Programme Avenir Lyon Saint-Etienne" of the Université de Lyon (ANR-11-IDEX-0007), within the Program "Investissements d'Avenir" operated by the French National Research Agency. The research leading to these results has received funding from the People Programme (Marie Curie Actions) of the European Union's Seventh Framework Programme (FP7/2007-2013) under REA grant agreement No. PCOFUND-GA-2013-609102, through the PRESTIGE programme coordinated by Campus France. The authors are grateful to the reviewer for his insightful comments that led to an improvement of the paper. Prof. G. Parisi is kindly acknowledged for very valuable hints and discussions.

REFERENCES

[1] Krause J. and Ruxton G., *Living in Groups* (Oxford University Press) 2002.
[2] Couzin I. and Krause J., *Adv. Study Behav.*, **32** (2003) 1.
[3] Dyer J., Johansson A., Helbing D., Couzin I. and Krause J., *Philos. Trans. R. Soc. London, Ser. B: Biol. Sci.*, **364** (2009) 781.
[4] Vicsek T. and Zafeiris A., *Phys. Rep.*, **517** (2012) 71.
[5] Arganda S., Pérez-Escudero A. and de Polavieja G., *Proc. Natl. Acad. Sci. U.S.A.*, **109** (2012) 20508.
[6] De Lellis P., Polverino G., Ustuner G., Abaid N., Macrì S., Bollt E. and Porfiri M., *Sci. Rep.*, **4** (2014).
[7] Jeschke J. and Tollrian R., *Oikos*, **111** (2005) 547.
[8] Zheng M., Kashimori Y., Hoshino O., Fujita K. and Kambara T., *J. Theor. Biol.*, **235** (2005) 153.
[9] Ioannou C., Guttal V. and Couzin I., *Science*, **337** (2012) 1212.
[10] Svendsen J., Skov J., Bildsoe M. and Steffensen J., *J. Fish Biol.*, **62** (2003) 834.
[11] Johansen J., Vaknin R., Steffensen J. and Domenici P., *Mar. Ecol. Prog. Ser.*, **420** (2010) 221.
[12] Hemelrijk C., Reid D., Hildenbrandt H. and Padding J., *Fish Fish.*, **16** (2015) 511.
[13] Lindauer M., *Nature*, **179** (1957) 63.
[14] Franks N., Pratt S., Mallon E., Britton N. and Sumpter D., *Philos. Trans. R. Soc. London, Ser. B: Biol. Sci.*, **357** (2002) 1567.
[15] Couzin I., Krause J., Franks N. and Levin S., *Nature*, **433** (2005) 513.
[16] Ward A., Sumpter D., Couzin I., Hart P. and Krause J., *Proc. Natl. Acad. Sci. U.S.A.*, **105** (2008) 6948.
[17] Couzin I., *Trends Cogn. Sci.*, **13** (2009) 36.
[18] Nagy M., Ákos Z., Biro D. and Vicsek T., *Nature*, **464** (2010) 890.

[19] Leonard N., Shen T., Nabet B., Scardovi L., Couzin I. and Levin S., *Proc. Natl. Acad. Sci. U.S.A.*, **109** (2012) 227.
[20] Ballerini M., Cabibbo N., Candelier R., Cavagna A., Cisbani E., Giardina I., Lecomte V., Orlandi A., Parisi G., Procaccini A. *et al.*, *Proc. Natl. Acad. Sci. U.S.A.*, **105** (2008) 1232.
[21] Puckett J., Kelley D. and Ouellette N., *Sci. Rep.*, **4** (2014) 4766.
[22] Abaid N., Bartolini T., Macri S. and Porfiri M., *Behav. Brain Res.*, **233** (2012) 545.
[23] Purcell E., *Am. J. Phys.*, **45** (1977) 3.
[24] Couzin I., Krause J., James R., Ruxton G. and Franks N., *J. Theor. Biol.*, **218** (2002) 1.
[25] Succi S., *EPL*, **109** (2015) 50001.
[26] Peskin C., *Acta Numer.*, **11** (2002) 479.
[27] Feng Z.-G. and Michaelides E., *J. Comput. Phys.*, **195** (2004) 602.
[28] Becker L., Koehler S. and Stone H., *J. Fluid Mech.*, **490** (2003) 15.
[29] Liu J., Weller G., Zern B., Ayyaswamy P., Eckmann D., Muzykantov V. and Radhakrishnan R., *Proc. Natl. Acad. Sci. U.S.A.*, **107** (2010) 16530.
[30] Ayyaswamy P., Muzykantov V., Eckmann D. and Radhakrishnan R., *J. Nanotechnol. Eng. Med.*, **4** (2013) 011001.